

<https://doi.org/10.1038/s41529-024-00454-w>

Organic carbon source controlled microbial olivine dissolution in small-scale flow-through bioreactors, for CO₂ removal

Check for updates

Thomas D. W. Corbett¹✉, Marcus Westholm¹, Anna Rosling², Tullia Calogiuri^{3,4}, Reinaldy Poetra⁵, Harun Niron^{6,7}, Mathilde Hagens⁴, Alix Vidal³, Jan Willem Van Groenigen³, Jens Hartmann⁵, Ivan A. Janssens⁶, Lukas Rieder⁵, Eric Struyf⁶, Michiel Van Tendeloo⁸, Siegfried E. Vlaeminck⁸, Sara Vicca^{6,7} & Anna Neubeck¹

The development of carbon dioxide removal methods, coupled with decreased CO₂ emissions, is fundamental to achieving the targets outlined in the Paris Agreement limiting global warming to 1.5 °C. Here we are investigating the importance of the organic carbon feedstock to support silicate mineral weathering in small-scale flow through bioreactors and subsequent CO₂ sequestration. Here, we combine two bacteria and two fungi, widely reported for their weathering potential, in simple flow through bioreactors (columns) consisting of forsterite and widely available, cheap organic carbon sources (wheat straw, bio-waste digestate of pig manure and biowaste, and manure compost), over six weeks. Compared to their corresponding abiotic controls, the inoculated straw and digestate columns release more total alkalinity (~2 times more) and produce greater dissolved and solid inorganic carbon (29% for straw and 13% for digestate), suggesting an increase in CO₂ sequestration because of bio-enhanced silicate weathering. Microbial biomass is higher in the straw columns compared to the digestate and manure compost columns, with a phospholipid fatty acid derived total microbial biomass 10 x greater than the other biotic columns. Scanning Electron Microscopy imaging shows the most extensive colonisation and biofilm formation on the mineral surfaces in the straw columns. The biotic straw and digestate columns sequester 50 and 14 mg C more than their abiotic controls respectively, while there is no difference in the manure columns. The selection of organic carbon sources to support microbial communities in the flow through bioreactors controls the silicate weathering rates and CO₂ sequestration.

Safe and scalable carbon dioxide removal methods (CDR) will be required to meet the goal of the Paris agreement to limit warming to well-below 2 °C^{1–5}. It has been estimated that CO₂ removal needs to reach 0.5 Gt CO₂ y⁻¹ by 2030, increasing to 5 Gt CO₂ y⁻¹ by 2050, and 10 Gt CO₂ y⁻¹ by 2100^{3,6}. Enhanced silicate weathering is one of the

proposed CDRs, with an estimated climate change mitigation potential of 2–4 Gt CO₂ y⁻¹⁷. Silicate weathering buffers atmospheric CO₂ partial pressure, balancing emissions over geologic timescales thereby stabilising the climate to habitable conditions^{8,9}. Enhanced silicate weathering, based on the acceleration of natural microbial silicate

¹Department of Earth Sciences, Uppsala University, Villavägen 16, Uppsala, Sweden. ²Department of Ecology and Genetics, Uppsala University, Norbyvägen 18, Uppsala, Sweden. ³Soil Biology Group, Department of Environmental Sciences, Wageningen University and Research, Droevendaalsesteeg 3a, 6708 PB Wageningen, The Netherlands. ⁴Soil Chemistry and Chemical Soil Quality, Department of Environmental Sciences, Wageningen University and Research, Droevendaalsesteeg 3a, 6708 PB Wageningen, the Netherlands. ⁵Institute for Geology, Center for Earth System Research and Sustainability, University of Hamburg, Bundesstrasse 53, Hamburg, Germany. ⁶Plants and Ecosystems (PLECO), Biology Department, University of Antwerp, Universiteitsplein 1, 2610 Wilrijk, Belgium. ⁷Department of Bioscience Engineering, University of Antwerp, Groenenborgerlaan 171, 2610 Wilrijk, Belgium. ⁸Research Group of Sustainable Energy, Air and Water Technology, Department of Bioscience Engineering, University of Antwerp, Groenenborgerlaan 171, Antwerpen, Belgium.

✉ e-mail: corbett.tdw@gmail.com

weathering processes, could have the potential to significantly mitigate climate change^{5,10}.

Silicate weathering is a natural process whereby silicate minerals are dissolved in the presence of water and CO₂, subsequent precipitation of carbonate minerals can provide long term storage of CO₂¹¹. Biota play an important role in the silicate weathering cycle. Biological processes can complement physical and chemical processes to mobilise nutrients from within minerals¹². Approximately 90% of terrestrial plant species form symbiotic relationships with mycorrhizal fungi¹³, supplying organic carbon to their symbiotic partners in exchange for water and nutrients that the fungus take up after release from organic and mineral substrate in soil, including from silicate rocks during dissolution¹⁴. Further, many free-living saprotrophic fungi can also access nutrients from organic matter¹⁵. Plant roots may stimulate dissolution through improving soil structure and hydrology¹⁶. Earthworms can increase mineralisation and mineral dissolution, through the ingestion of soil particles and fresh residues¹⁷.

Dissolution of silicate minerals in the presence of atmospheric CO₂ results in the formation of alkalinity (Fig. 1). The subsequent precipitation of carbonate minerals in the soil or receiving waters, as calcium carbonate for example, provides longer-term stable storage of CO₂¹¹. Silicate weathering is driven by a range of abiotic and biotic processes (to support nutrient uptake). Microbial silicate weathering is attributed to: (i) oxidoreduction; (ii) acidolysis; (iii) chelation/siderophores (complexolysis); and, (iv) physical disruption^{18–21} (Fig. 2).

In oxidoreduction reactions, microorganisms can meet their metabolic/energetic needs by utilising alternative electron acceptors, such as nitrate and sulfate, instead of oxygen as the electron acceptor¹⁸. Insoluble iron (Fe³⁺) within minerals can also be used, however, direct contact (e.g.,

biofilms) with the mineral surface is required for electron transfer via excreted and/or membrane-associated molecules^{18,22–25}. Minerals are susceptible to dissolution in the presence of inorganic and organic acids, and more complex molecules produced by microorganisms^{18,26}. Organic acids and chelators such as siderophores, can drive mineral dissolution through, (i) adherence to mineral surfaces and nutrient extraction via electron transfer, (ii) breaking oxygen links, and (iii) creating cation/anion concentration imbalances via chelation through their carboxyl and hydroxyl groups²⁷. The production of CO₂ during microbial respiration can produce carbonic acid, stimulating further mineral weathering²⁸. Physical weathering via the formation of new cracks/fissures in mineral/rocks, due to increased pressures induced by fungal colonisation of, and hyphae growth in, rock particle depressions, pores and mineral cleavage planes has been postulated^{19–21}. Microbial/rock weathering interactions are already taken advantage of in industrial processes, particularly in biomining where microbes have been used in the bioleaching of Cu, Co, Ni, Zn, U, and Au^{29,30}.

Microbial silicate weathering has been extensively investigated^{25,31–35}, but the focus has not been on the CDR potential. Most studies have focused, however, on the *in natura* silicate weathering and the effects on soil biota^{36,37}, or single microorganisms with specific growth media combined with relatively small masses of minerals^{25,31,32,38,39}. Flow through bioreactor experiments with one or two fungi or bacteria, supplied with specific nutrient media, have produced mixed results in terms of enhanced mineral dissolution^{38,40}. There remains a need to establish the weathering ability of fungi and bacteria under non-optimal (e.g., low temperature, and without specific nutrient media) bioreactor conditions, for the development of *ex natura* CDRs to sequester CO₂ at low energy cost. Here, we sought to enhance the weathering of forsterite to promote inorganic carbon

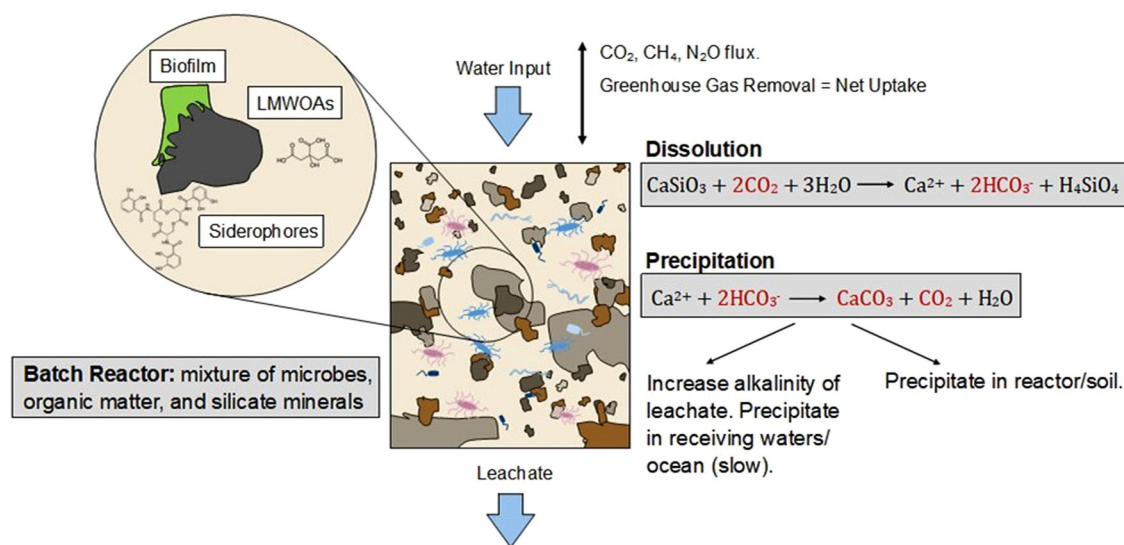


Fig. 1 | Simplified summary of silicate weathering, and microbial processes/mechanisms which promote silicate weathering—in the flow through bioreactors (columns).

Fig. 2 | Column schematic. **A** Filled column with leachate collected in lower chamber. **B** The underside of the upper chamber. **C** Upper chamber with nylon mesh (20 μm) installed.

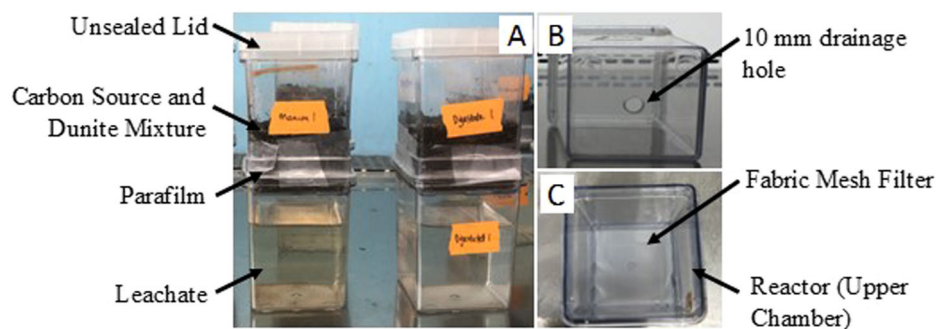


Table 1 | Experimental setup and number of replicates

	Carbon Source		
	Straw	Digestate	Manure Compost
Biotic	3	3	3
Abiotic Control	3	3	3

sequestration, though the combination of fungi and bacteria, and widely available organic carbon sources.

Methods and materials

Eighteen flow-through (Table 1) bioreactors (referred to as columns henceforth) containing 200 g of dunite with 5 g of one of three organic carbon sources were used. Half of the columns were inoculated with a combination of two bacteria and two fungi. The following sections detail the mineral, microbes, organic carbon sources, experimental setup, and analyses utilised.

The rock chosen for this experiment was dunite (Sibelco, Norway), containing 95% forsterite (composition of $Mg_{1.86}Fe_{0.14}SiO_4$)⁴¹, with a grain size of 1 mm ($d_{80} = 937.51 \mu m$) and a BET (Quantachrome Autosorb iQ, USA) determined surface area of $1.128 \pm 0.005 m^2 g^{-1}$. The three organic carbon sources utilised were wheat straw, digestate, and manure compost (details are provided in section “Experimental setup”).

The dunite consisted of primarily forsterite olivine (Mg_2SiO_4) rather than fayalite olivine (Fe_2SiO_4), henceforth olivine was used synonymously for dunite and forsterite.

Bacteria and fungi selection

The selection of the microbes was based on the following criteria: (i) the ability to grow on solid surfaces, and/or form biofilms⁴²; (ii) documented ability to interact with mineral/rock surfaces and/or bioleach⁴²; and, (iii) being non-pathogenic/safe to use. The fungi selected were *Knufia petricola* A95 (*K. petricola*) (Westerdijk Fungal Biodiversity Institute, Netherlands), and *Aspergillus niger* (DSM 821 - Doelger 2) (Leibniz Institute, Germany). The bacteria selected were *Bacillus subtilis* (NCBI 3610) (*B. subtilis*), and *Cupriavidus metallidurans* (type strain CH34) (*C. metallidurans*) (Leibniz Institute, Germany).

Knufia petricola is a non-pathogenic, extremotolerant, and rock-inhabiting fungus⁴³, which has been reported to enhance the weathering of olivine^{33,38}. *K. petricola* have been shown to form biofilm layers that sequestered significant amounts of Fe, thereby preventing the formation of the weathering limiting Fe hydroxides at the mineral surface^{33,38}.

Aspergillus niger has been reported to weather biotite, through the formation of fungal-mineral aggregates and organic acids (e.g., citric acid and oxalic acid), resulting in the release of potassium, magnesium and iron³⁹. *A. niger* is a filamentous fungus, widely used for the production of food grade acids (e.g., citric acid), enzymes and secondary metabolites⁴⁴.

Bacillus subtilis is a soil bacterium widely distributed in various environments, capable of causing physical and chemical breakdown of granite substrate, with plagioclase composing minerals showing increased vulnerability compared to biotite³¹. Granite weathering was influenced by the formation of etch pits, and despite an unknown mechanism for the increased weathering by *B. subtilis*, localised changes in pH was observed in the experiments, which may have influence the surface alteration³¹. *B. subtilis* weathering interactions with basalt have also been investigated with mixed results⁴².

Cupriavidus metallidurans is a heavy metal-resistant bacterium, which has been widely investigated for its weathering potential of basalts^{25,42,45}. *C. metallidurans* promotes rock weathering through the up-regulation of porins and transporters associated with biofilm formation, changing the microbe-mineral surface chemical equilibrium, reducing the Fe saturation state^{25,42,45}. Both *B. subtilis* and *C. metallidurans* are risk group 1, under the Technical Rules for Biological Agents⁴⁶.

Table 2 | Major element and nutrient composition of the organic carbon sources

	Component (mg/g)							
	Ca	Fe	K	Mg	Zn	C	N	P
Straw	2.83	0.11	8.10	0.48	0.00	452.1	4.3	0.48
Digestate	9.79	0.96	2.75	1.22	0.13	447.1	9.2	3.70
Manure Compost	19.55	4.44	2.3	2.73	0.06	433.6	13.5	1.52

Culturing

Cultures were received freeze dried and were subsequently rehydrated and propagated following the supplier instructions. 100 mL of growth media solution was transferred into 500 mL Erlenmeyer flasks, which were stoppered and sealed with aluminium foil prior to autoclaving at 121 °C for 20 min, and then allowed to cool prior to inoculation. New cultures were prepared by transferring a hundredth volume of the culture to fresh media^{38,47}. All reagents were purchased from Merc (Sweden).

K. petricola (Westerdijk Institute, The Netherlands) was grown in a malt extract broth (MEB), containing 2% (w/v) malt extract, 0.1% (w/v) casein-digested peptone, and 2% (w/v) D-(+)-glucose, in MilliQ (18.2 mΩ) water^{33,38,48}. *A. niger* (Leibniz Institute, Germany) was grown in potato dextrose broth (PDB). The PDB was prepared by gently boiling 200 g of cleaned and sliced potatoes in 500 mL of MilliQ water for 60 min, before sieving and collecting the potato extract solution. 10 g of D-(+)-glucose was dissolved in the extract solution, and subsequently made to 500 mL with MilliQ water. Both fungi were grown at room temperature, on an orbital shaker, in darkness. A sterile kitchen blender was used to disaggregate the cultures by pulsing gently, to avoid heat generation.

B. subtilis and *C. metallidurans* (Leibniz Institute, Germany) were grown on nutrient broth (DSMZ media 1). The nutrient broth was prepared by dissolving 5.0 g peptone, 3.0 g NaCl, and 3.0 g meat extract in MilliQ (1000 mL). The pH was adjusted to 7.0 using 1 mol L⁻¹ NaOH and HCl. Both bacteria were grown at 30 °C, in darkness on an orbital shaker at 30 rpm.

Organic carbon sources

Three widely available organic carbon sources were selected to support the microbial growth in the columns: wheat straw (Welkoop, The Netherlands); phosphorus depleted digestate of pig manure and biowaste (Groene Mineralen Centrale, The Netherlands); and manure compost (Weibulls, Sweden). The major components were determined via HR-ICP-MS (Thermo Element 2, Thermo Fisher Scientific, USA), upon a modified salicylic acid/sulfuric acid digestion (Table 2)⁴⁹. Total carbon and nitrogen were determined using an elemental analyser (FlashSmart, Thermo Fisher Scientific, USA), upon drying and grinding.

Nuclear magnetic resonance (¹³C NMR) was performed to provide further insight to the nature of the carbon compounds within the organic carbon sources. NMR methods and results were included in the Supplementary Information. There was little difference in the ¹³C NMR of the wheat straw and the digestate, while the ¹³C NMR of the manure compost indicated increased the presence of aldehyde C=O, and potentially alkene C=C, compared to the digestate and wheat straw.

Experimental setup

The columns consisted of 200 g of dunite (olivine) and 5 g of the respective organic carbon source (wheat straw, digestate, and manure compost), which was well mixed. The straw was passed through a 6 mm grinder. The dunite and organic carbon sources were dried at 40 °C for 24 h prior to weighing and mixing. Upon weighing and mixing, the dunite and organic carbon source mixes were autoclaved three times at 121 °C for 30 min to sterilise the columns and the mixtures in each column. The inoculated columns were stored separately to the abiotic control columns, and each set of columns

(abiotic and inoculated) were worked upon separately under sterile conditions.

A mixed inoculum was prepared by sieving (20 µm nylon mesh filter) the fungal cultures to remove the bulk of the liquid, and mixing with 50 mL of each bacteria culture in a 500 mL beaker, before blending gently with a sterile kitchen blender, pulsing to avoiding heating the mixture. In total 6 columns were prepared for each organic carbon source, 3 control and 3 inoculated (with 10 mL each) columns.

The columns were watered with 50 mL of autoclaved distilled water (pH 5.0) using a volumetric flask, daily from Monday to Friday for 6 weeks. Leachate was collected in the bottom chamber over each week and removed for analysis before watering began at the start of each week. For weeks 5 and 6 the watering schedule of the inoculated straw columns had to be altered (150 mL total rather than 250 mL), due to the growth of *A. niger* over the filter membrane which slowed the water flow through rate and caused the column to flood. This change in flow was factored into subsequent leachate analyses and calculations.

Solid samples (two per column) were collected from the column at the end of the 6 weeks, after homogenisation of each column. Samples for were placed in sterile 50 mL DNA/RNA free centrifuge tubes, and stored at $-20\text{ }^{\circ}\text{C}$ for PLFA and solid carbon analyses.

Geochemical analyses

The leachate was analysed weekly for pH, alkalinity, conductivity, and dissolved organic and inorganic carbon (DOC and DIC). Filtered samples were frozen for low molecular weight organic acids, and major cations and anions. Samples were filtered to 0.25 µm using polyethersulfone filters (Fisherbrand, USA), prior to analysis.

The pH and conductivity of the leachate was determined using pH and conductivity probes. Alkalinity was determined via manual end point titration (Piston Burette E 274, Metrohm, Switzerland) of 40 mL of leachate to pH 4.5 with 0.02 mol L⁻¹ HCl while stirring. DOC and DIC analyses were performed using a Sievers M9 (General Electric, USA). Due to the high organic carbon concentrations, samples from weeks 1 and 2–3 were diluted gravimetrically (1:20 and 1:10, respectively) for DOC and DIC analysis, to remain within the quantification window.

Low molecular weight organic acids (LMWOAs), and the major cations and anions were determined via ion chromatography (Metrohm ion chromatography system 883 basic IC Plus). A Metrosep A Supp 5 (250 × 4.0 mm) separation column was used for the citrate, oxalate, acetate and the major anions (NO₃⁻, SO₄²⁻, PO₄³⁻, Cl⁻, and F⁻) analyses. The oxalate, acetate and anion analyses utilised 3.2 mmol L⁻¹ Na₂CO₃ and 1.0 mmol L⁻¹ NaHCO₃ as the eluents. Citrate analyses were performed separately using 4.5 mmol L⁻¹ NaOH and 14.5 mmol L⁻¹ Na₂CO₃ eluent solutions. A Metrosep C6 (250 × 2.0 mm) separation column and 4.0 mmol L⁻¹ nitric acid and 1.0 mmol L⁻¹ dipicolinic acid eluent solutions were utilised for cation (Na⁺, K⁺, Mg²⁺, Ca²⁺, and NH₄⁺) analyses.

The column contents were analysed for solid organic and inorganic carbon (SOC and SIC) via loss of ignition and elemental analysis respectively (Costech Instruments ECS 4010). Briefly, subsamples from the homogenised columns (and an unreacted mineral blank) were oven dried at 105 °C for 24 h. The samples were allowed to cool in a desiccator, after which they were ground at 650 rpm for 10 min in a ball mill (Retsch PM 100 CM). For each ground sample 10 g were weighed into muffled ceramic crucibles, and combusted at 550 °C for 3 h, before reweighing. SOC was calculated as the loss of mass due to combustion upon conversion using the weight percentage of carbon in the carbon source (Table 2). Subsamples of the combusted samples were taken (~20 mg), for SIC (sequestered inorganic carbon) analysis via combustion in an elemental analyser. A series of acetonitrile standards (71.09% carbon) were used produce a calibration curve, alongside EDTA and high organic carbon sediment quality controls.

Scanning electron microscopy (SEM)

A glutaraldehyde, ethanol gradient and bis(trimethylsilyl)amine (HMDS) method was used to fix the fungal and bacteria cells, to prevent collapse of

the cells and maintain the structural integrity of the biofilms prior to SEM. Briefly, excess water was removed from the samples under vacuum using a 0.8 µm membrane filter. The 0.8 µm membrane filters were placed in 40 mL of glutaraldehyde (0.16 mol L⁻¹) and phosphate buffer (0.1 mol L⁻¹), covered with parafilm, and left for 4 h. The filters were then placed in phosphate buffer solution (0.1 mol L⁻¹) for 10 min, twice, prior to drying via an ethanol gradient. The ethanol gradient used was 50, 70, 80, 90, 95, 100, 100, and 100% v/v. The filters were then placed in HMDS for 5 min, and left to air dry overnight.

SEM measurements of palladium coated samples was performed, using a Zeiss Supra 35 VP (Carl Zeiss SMT, Oberkochen, Germany) field emission SEM, on the organic carbon sources, minerals, and samples from the columns after the experiment, was performed to visualise the colonisation of the organic carbon sources and mineral grains by the bacteria and fungi, as well as the structural changes of the organic carbon sources and mineral.

PLFA extraction and analysis

The PLFA extraction involved three steps, firstly extraction, then lipid fractionation, and finally alkaline methanolysis. All vials and glass pipettes were muffled at 500 °C for 3 h before use. A solid sample for each column, collected at the end of the experiment, was freeze dried prior to extraction.

Bligh and Dyer reagent (5 mL) was added to 6 g of freeze-dried sample in a 10 mL glass vial (vial 1), then vortexed briefly and left to stand for 2 h. The samples were then centrifuged, and the supernatant was removed to separate clean 25 mL glass vials (vial 2). These extraction steps were repeated three times, i.e., 5 mL of Bligh and Dyer reagent were added vial 1, then vortexed, left to stand and centrifuged before the supernatant was collected in vial 2. Citrate buffer (4 mL of 0.16 mol L⁻¹) and chloroform (4 mL of >99.5%) were added to the extractant (vial 2), before vortexing and leaving to stand overnight. A total of 4.5 mL of lipid extractant was transferred to 1.5 mL vials, and evaporated under a nitrogen stream at 40 °C (1.5 mL at a time).

Bond Elut SPE columns (Agilent, USA), one per sample, were placed in a vacuum manifold and conditioned with 1 mL of chloroform (>99.5%). Chloroform (100 µL of >99.5%) was added to the dried samples, vortexed gently, and transferred to the individual SPE columns (repeated three times), before applying vacuum. Chloroform (1.4 mL of >99.5%) was added to remove the neutral lipids, followed by three 1.5 mL acetone (>99.5%) washes to remove the glycolipids. Methanol (1 mL of >99.5%) was added to the SPE column, to remove the phospholipids, and collected in muffled vials and evaporated under nitrogen at 40 °C (repeated three times).

Alkaline methanolysis was performed by briefly vortexing the samples with 0.2 mL of concentrated methanol and toluene solution (1:1), followed by incubation for 15 min at 37 °C. The samples were cooled and 0.4 mL of a hexane and chloroform solution (4:1), 0.06 mL acetic acid (1 mol L⁻¹), and 0.4 mL of MilliQ water were added, followed by further vortexing. The samples were left to stand for 2 h for the phases to separate, before the upper organic phase was transferred to separate muffled vials and evaporated under nitrogen at room temperature. The vials were sealed with PTFE caps, and stored at $-20\text{ }^{\circ}\text{C}$ before dissolution in 0.15 mL of hexane and analysis via GCMS.

Fungal and Bacterial Acid Methyl Ester (FAME and BAME) mixes were used to identify the peaks, and a nonadecanoate internal standard was used to calibrate the peaks. PLFA analyses alone were utilised to measure the total biomass given that peaks 14:0, 15:0, 16:0, and 17:0 occur in all microorganisms and should sufficiently capture combined fungal and bacterial biomasses⁵⁰. Further, *Aspergillus Niger* can be saprophytic, and gram positive and gram negative bacteria, are well accounted for in the PLFA standards^{50,51}.

Weathering rate

The calculated weathering rates represent an average rate for the whole column, accounting for non-linear chemical gradients through the column due to the flow through transport of reaction products⁵², and potential non-homogenous biotic weathering effects. Weathering rate was calculated as

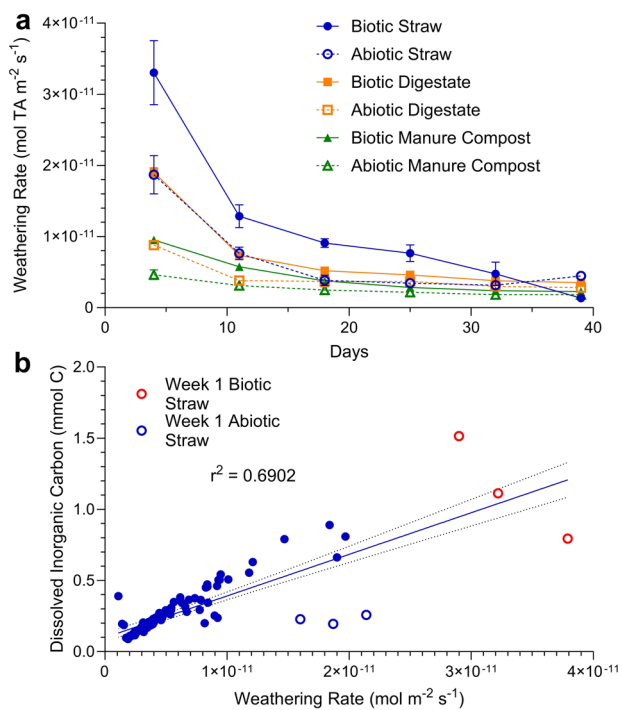


Fig. 3 | Weathering rate and dissolved inorganic carbon through time. **a** Average weathering rate for each sampling period, calculated as total alkalinity release. **b** Dissolved inorganic carbon versus weathering rate. Error bars represent standard deviation.

total alkalinity release rate. Weathering rates calculated on the release of individual cations (for example Mg^{2+}) may misrepresent the weathering rate, due to their potential to add significantly to the cation binding potential for alkalinity production⁵². Experiments using the same olivine (dunite) found that while Mg^{2+} constituted 99% of the cations in the fresh material, the cumulative released fraction of Mg^{2+} was 14% ($Ca^{2+} = 23%$, $Na^+ = 32%$, and $K^+ = 32%$) over 300 days⁵².

The release rate of the total alkalinity (R) was calculated in $mol\ m^{-2}\ s^{-1}$, using Eq. 1, where Q was the outflux volume (L) from the column per time step t (s), C was the total alkalinity concentration ($mol\ L^{-1}$) at time t, m was the material mass in the column (g), A was the specific surface area ($m^2\ g^{-1}$), and τ (s) was the residence time of the solution occupying the material pore space⁵².

$$R = \frac{Q_t \times C_t}{m \times A \times \tau} \quad (1)$$

Residence time was calculated using Eq. 2, where V_c was the column volume occupied with mineral (m^3), V_o was the outflow volume (m^3), m_c was the initial mass of the starting material (g), p was the material specific density ($g\ m^{-3}$) for time t (s)⁵².

$$\tau = \frac{V_c - \frac{m_c}{p}}{V_o} \times t \quad (2)$$

Statistical analyses

All statistical analyses were performed using PRISM 9.5.0 (GraphPad Software, USA). Standard deviation ($n = 3$) was calculated for all replicates and is provided in the tables and graphs. Where accumulative averages were calculated, the values for each individual column were summed, before being averaged with their replicates and the standard deviation calculated.

Repeated measures two-way analysis of variance (ANOVA) tests was performed to determine the effect of time and column composition

(inoculation and organic carbon source) on dissolved inorganic carbon, and weathering rate. A standard ANOVA test was performed to determine the effect of column composition on total inorganic carbon. Tukey’s test was performed to determine the significance of difference between groups, for $p < 0.05$. Pearson correlation was computed to determine the relationship between dissolved inorganic carbon and weathering rate.

Results

Total Alkalinity release rate and weathering

Weathering rates, based on total alkalinity released to the leachate, decrease through time for all columns (Fig. 3a). All the biotic weathering rates were about 2 times their abiotic control, the largest enhancement of weathering rate, compared to the abiotic controls, was in columns utilising straw ($1.43 \times 10^{-11}\ mol\ m^{-2}\ s^{-1}$ larger at day 4 and $4.21 \times 10^{-12}\ mol\ m^{-2}\ s^{-1}$ larger at day 25). The weathering rates for the biotic and abiotic straw columns converged between day 32 and 39, with the abiotic weathering rate becoming larger by day 39, likely due to the reduced volume applied to the biotic straw columns over that period due to clogging. The weathering rate for the biotic and abiotic digestate columns at day 4 were 1.90×10^{-11} and $8.79 \times 10^{-12}\ mol\ m^{-2}\ s^{-1}$, decreasing to 3.52×10^{-12} and $2.83 \times 10^{-12}\ mol\ m^{-2}\ s^{-1}$ respectively at day 39. The biotic and abiotic manure compost columns produced weathering rates at day 4 of 3.75×10^{-12} and $2.48 \times 10^{-12}\ mol\ m^{-2}\ s^{-1}$ respectively, decreasing to 2.26×10^{-12} and $1.83 \times 10^{-12}\ mol\ m^{-2}\ s^{-1}$ by day 39.

There was a strong relationship ($R^2 = 0.6902$) between weathering rate and dissolved inorganic carbon (Fig. 3b), which increases in strength ($R^2 = 0.8124$) when the outliers (abiotic straw day 4) are removed. The correlation between weathering rate and dissolved inorganic carbon provided Pearson r values of 0.8308 and 0.9013, respectively, with two-tailed $p < 0.0001$ (Pearson’s correlation). Suggesting there is a strong statistical relationship between weathering rate and dissolved inorganic carbon, that is not due to random sampling. Repeated measures ANOVA test of the importance of time and column composition, to weathering rate, determined that the interaction between time and column composition accounted for 26.1% of the total variation in the weathering rate ($P < 0.0001$), while time and column composition accounted for 54.1% ($P < 0.0001$) and 21.2% ($P < 0.0001$) of the total variation respectively (P values from Two-way ANOVA).

Carbon and Alkalinity

The biotic columns generally sequestered more carbon than their corresponding abiotic controls both as solid and dissolved inorganic carbon (Table 3). The biotic straw produced ~50 mg more inorganic carbon than the abiotic straw, and ~101 mg more than biotic digestate, the next best biotic system. The production of inorganic carbon was as follows: biotic straw > abiotic straw > biotic digestate > abiotic digestate > abiotic manure compost \geq biotic manure.

All biotic columns produced more inorganic carbon and alkalinity than their abiotic controls (Table 3 and Fig. 4). The biotic straw columns produced the most DIC and alkalinity, and showed the greatest difference to the respective abiotic control columns (~50 mg C).

Based on the repeated measures two-way ANOVA analysis, the interaction between time and the column composition (biotic/abiotic, and organic carbon source) accounted for 5.2% of the total variance in dissolved inorganic carbon. The interaction was extremely significant ($P < 0.0001$). Time accounts for 31.6% of the total variance ($P < 0.0001$), and the column composition accounts for 61.0% of the total variance ($P < 0.0001$) in dissolved inorganic carbon (P values from Two-way ANOVA). The Tukey’s multiple comparisons test determined that there was a statistically significant difference in production dissolved inorganic carbon between all the columns, except between the abiotic digestate columns and the abiotic straw columns, and the abiotic digestate columns and abiotic manure columns.

The ANOVA analysis of the effect the organic carbon source and inoculation status on the total inorganic carbon determined that the

Table 3 | Average total solid organic (SOC) and inorganic carbon (SIC), dissolved organic and inorganic carbon (DIC), and total inorganic carbon (TIC) with standard deviation, produced over the 6 weeks

	SOC (g)	SIC (mg)	DOC (mg)	DIC (mg)	Δ TIC* (mg)
Biotic Straw	1.06 ± 0.14	307.0 ± 21.9	172.9 ± 9.8	35.2 ± 5.7	224.4 ± 22.8
Abiotic Straw	0.97 ± 0.15	276.0 ± 15.9	154.3 ± 6.2	15.5 ± 1.5	173.7 ± 16.2
Biotic Digestate	0.97 ± 0.10	218.1 ± 10.4	55.1 ± 2.4	22.9 ± 1.2	123.2 ± 10.8
Abiotic Digestate	0.96 ± 0.19	214.1 ± 14.9	75.5 ± 3.5	12.8 ± 1.3	109.1 ± 15.2
Biotic Manure Compost	1.11 ± 0.48	186.5 ± 2.1	37.3 ± 0.8	16.2 ± 0.9	84.8 ± 3.6
Abiotic Manure Compost	0.71 ± 0.41	193.0 ± 21.9	42.7 ± 1.4	9.9 ± 0.6	85.3 ± 22.1
Olivine (unreacted)		117.8 ± 2.8			

Time and column Composition ANOVA - Source of Variation	% of total	P value
Interaction	5.2	<0.0001
Reactor Composition	61.0	<0.0001
Time	31.6	<0.0001
Inoculation Status and Organic Carbon Source ANOVA- Source of Variation		
Interaction	4.1	0.0538
Organic Carbon Source	84.8	<0.0001
Inoculation Status	4.5	0.0148

Summary of 2-Way ANOVA results.

*TIC equals the sum of SIC and DIC, minus the SIC of the unreacted olivine.

interaction between inoculation status and the organic carbon source accounted for 4.1% of the total variance, the interaction was not quite significant ($P = 0.0538$). The inoculation status accounted for 4.5% of the total variance ($P = 0.0148$), and the organic carbon source accounted for 84.8% of the total variance ($P < 0.0001$) in the total inorganic carbon (P values from Two-way ANOVA).

Dissolved organic carbon (DOC), the labile organic carbon fraction, was used as a proxy for bioavailable carbon. The straw produced more DOC in comparison to both the digestate and manure compost, while the release of DOC decreased through time for all columns throughout the experiment (Fig. 4c). The SOC was similar in all columns at the completion of the experiment (Table 3).

Microbial growth

Microbial growth was greatest in the columns which utilised straw (straw > digestate > manure compost) as the organic carbon source (Fig. 5 and Table 4). The fungi and bacteria more extensively colonised the organic carbon source and importantly the mineral grains (Fig. 5). Extensive biofilms were visible growing on mineral grains in the biotic straw columns, they were less extensive and more difficult to locate in the digestate and manure compost columns.

The PLFA peaks in the chromatograms were low for all samples, suggesting low total microbial biomass. The limited growth was likely due to the system becoming strongly nutrient limited by 25 days (Fig. 7). Growth was up to 23 times greater in the straw columns than in the other columns. Based on the repeated measures two-way ANOVA analysis, the interaction between the microbial species and the column composition (biotic/abiotic, and organic carbon source) accounted for 15.9% of the total variance in bacterial, fungal and total PLFA biomass, but was not significant ($P = 0.926$). The column composition and microbial taxa accounted for 41.2% ($P = 0.0005$) and 12.5% ($P = 0.0455$) of the total variance in bacterial, fungal and total PLFA biomass, respectively (P values from Two-way ANOVA). The large and significant effect of column composition on the total variance in PLFA biomasses suggests that the growth of the inoculated microbes depended most strongly on the organic carbon source.

LMWOAs

The LMWOAs tested were more abundant in the leachate from the straw columns compared to both the digestate and manure compost columns (Fig. 6). The increased organic acid mass in the straw leachate reflects the greater organic carbon mass in the leachate (Fig. 4). The acid mass trended down as the experiment progressed, converging as the masses approached zero, like the nutrient and ion masses in the leachate (Fig. 7 and Supplementary Fig. 2). The greater production of acetate and citrate in the abiotic straw columns suggested the breakdown of straw, and indeed all the carbon substrates, produced organic acids, independent of the microbial activity.

Nutrients

Nutrient masses (nitrogen, and phosphorus) present in the leachate generally trended down over the course of the experiment (Fig. 7), towards 0, suggesting the systems became heavily nutrient limited. This was most pronounced in the straw columns where nitrogen and phosphorus were close to 0 mg at 25 days.

Ammonium mass was indistinguishable between all the columns at each sampling period (3 mg at day 4, and 0 mg at day 39), despite the nitrogen differences present in the starting material (Table 2). Phosphate mass decreased for both the straw (~0.2–0.5 mg at day 4, to 0 mg at day 39) and digestate columns (~6 mg at day 4 to ~1.8 mg at day 39), while it remained stable in the manure compost columns, potentially reflecting the low microbial biomass (Table 4—PLFA) or stable dissolution from the manure compost. The phosphate present in the leachate of digestate columns was an order of magnitude greater than the straw and manure compost columns, reflecting the much higher phosphorus mass present in the digestate starting material (Table 2). The greater digestate phosphate mass did not result in increased microbial biomass and colonisation of mineral grains (Fig. 5 and Table 4). Nitrate mass decreased rapidly over the first 2 weeks, converging for all columns after 21 days. Nitrate mass present in the leachate was greater in the abiotic columns compared to their biotic counterparts (Fig. 7b).

The magnesium mass produced each week decreased throughout the experiment (Supplementary Fig. 2A), for both the biotic systems and their abiotic controls. The biotic systems, however, released more magnesium than their abiotic controls, with the greatest difference between the biotic

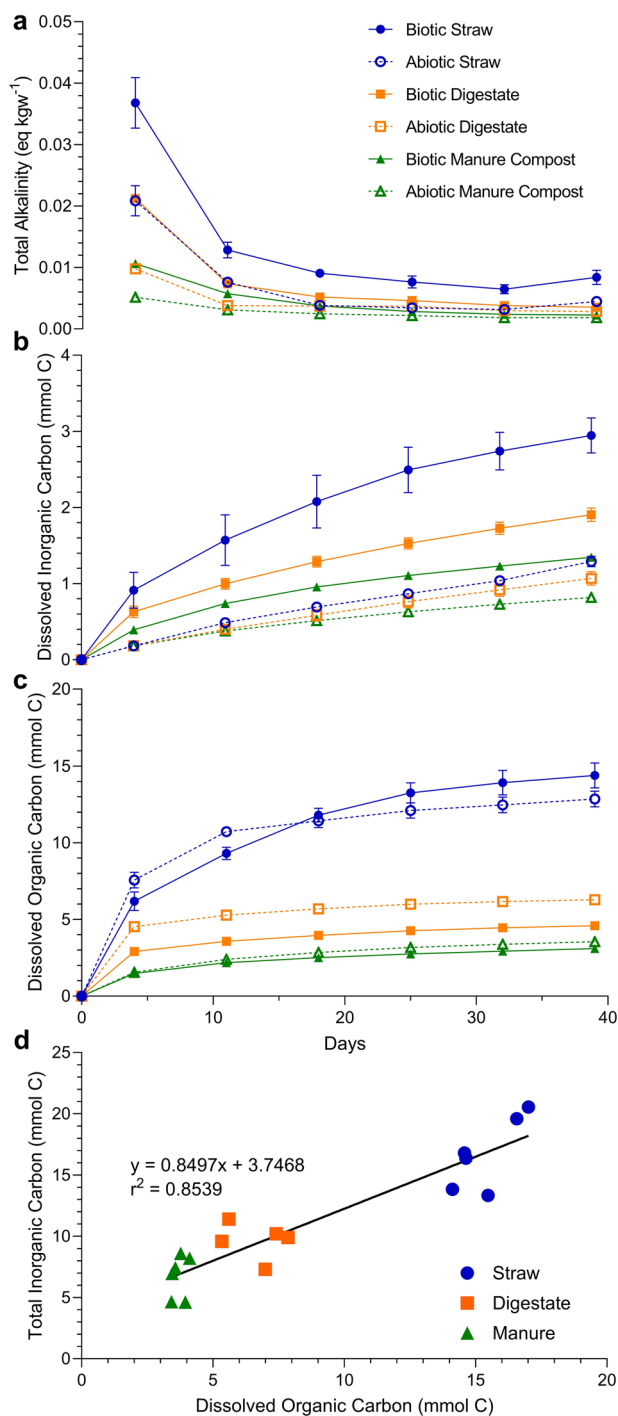


Fig. 4 | Alkalinity, dissolved inorganic carbon, and organic carbon through time. a Alkalinity, accumulative sums of (b) dissolved inorganic carbon and (c) dissolved organic carbon moles in the leachate, and (d) the total sequestered carbon versus the released organic carbon for each column. Error bars represent standard deviation.

and abiotic straw columns (~ 0.3 mmol at day 4, and 0.06 mmol at day 39). Similarly to the DIC/DOC and alkalinity (Fig. 4), there was considerable variance in the average magnesium mass in the first week for all systems which decreased as the experiment progressed.

There was little difference between the biotic and abiotic controls in the leachate calcium, sodium, and potassium masses (Supplementary Fig. 2). Initial spikes in the masses decreased rapidly in the first 3 weeks, approaching zero thereafter. The difference between the masses present in the leachate between organic carbon sources reflects their compositions

(Table 2). For example, the digestate columns produced about 20 mg of calcium more than the straw and manure columns in week 1, and have ~ 14 mg g^{-1} more calcium present in the starting material.

Discussion

Monitoring the release of appropriate olivine dissolution products can enable the determination of olivine dissolution rate^{53,54}, given the non-stoichiometric release of magnesium and other cations⁵², total alkalinity was used to calculate weathering rate. Total alkalinity release rate, and therefore weathering rate, decreased through time for all columns (Fig. 3a). The inoculated columns, however, released more total alkalinity in comparison to their abiotic controls, with the biotic straw column releasing the most. The effects of time (54.1% of total variation) and column composition (21.2% of total variation), and the interaction of time and column composition (26.1% of total variation), on the weathering rate were extremely significant ($P < 0.0001$ - from two-way ANOVA). Suggesting the mixed cultures of *Knufia petricola*, *Aspergillus niger*, *Bacillus subtilis* and *Cupriavidus metallidurans* enhanced the weathering of the forsterite olivine present in the dunite grains for all organic carbon sources but most significantly in the straw columns. Abiotic forsterite weathering rates are strongly pH dependent, with surface area normalised rates ranging from 10^{-7} to 10^{-12} from pH 1 to 12 at 25 °C¹¹. The weathering rates (3.3×10^{-11} maximum at 20 °C) in this experiment were similar to forsterite weathering rates (10^{-10} to 10^{-11}) at 25 °C and at comparable pH (7 to 8)¹¹. It is, however, difficult to compare weathering rates between experiments as experimental conditions (temperature, surface area, water flow through rate, etc) play a significant role in determining the weathering rate. The weathering rates reported here may underestimate the true weathering rate, given that cations released during weathering could enter the exchangeable pool in the material, increasing the cation exchange capacity and exchangeable bases which could lower total alkalinity⁵⁵.

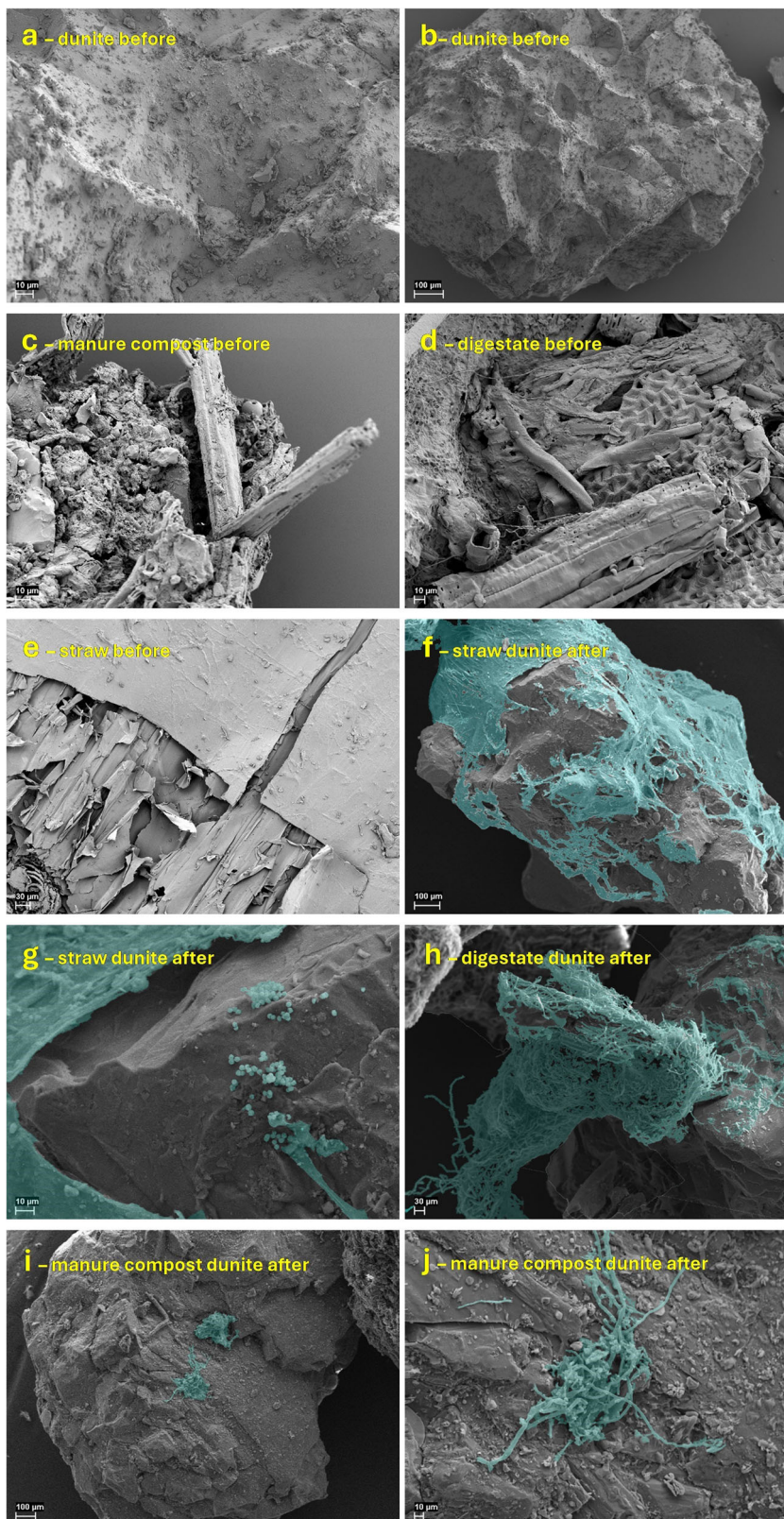
The total alkalinity released in the biotic straw columns was affected by a change in watering rate. Microbial growth on the filter of the biotic straw columns was so great, that the volume of water applied in weeks 5 and 6 was decreased to avoid overflow of the columns. This resulted in less leachate volume and therefore total alkalinity in the leachate, which in part may explain the sharp decrease in dissolution rate for the straw columns in week 5. In future experiments alterations to the column design are required to ensure clogging does not occur.

The contribution of organic alkalinity due to the presence of dissolved organic carbon to the total alkalinity was not determined. The contribution is typically considered negligible and not included in total alkalinity calculations⁵⁶, however, this could present errors in the weathering rates calculated here based on total alkalinity. Studies estuarine systems found organic alkalinity contributed between 0.3 and 12% to total alkalinity, however, there was not a strong relationship between dissolved inorganic carbon and organic alkalinity⁵⁷. Future studies comparing the effect of different carbon sources on mineral weathering should include potentiometric titrations⁵⁸, and carbon source controls to better estimate the contribution of dissolved organic species to total alkalinity.

The presence of microbes increased weathering of the olivine in comparison to abiotic controls ($\sim 100\%$ increase), even as weathering rate decreases through time overall. This was most pronounced in the straw columns where the weathering rate increased by 1.43×10^{-11} mol m^{-2} s^{-1} in the biotic columns than the abiotic controls at 4 days, decreasing to 4.21×10^{-12} mol m^{-2} s^{-1} greater after 25 days. Microbial weathering studies of artificially aged minerals in natural soils found a 30% increase in the dissolution of olivine in biotic experiments, and that although mineral-specific bacterial communities developed, the reactivity of aged powders was not restored⁵⁹.

The decrease in dissolution rate through the course of the experiment for all columns, suggests abiotic processes were the primary controls of the dissolution rate. The presence, however, of the microbes resulted in the release of more total alkalinity than the abiotic controls (Fig. 4), likely resulting from a slower decrease in the mineral weathering

Fig. 5 | Scanning electron microscopy (SEM) of the materials before and after weathering. SEM images before experiment: (a) and (b) dunite (olivine) mineral grain; (c) manure compost; (d) digestate; and (e) straw. SEM images of the mineral grains at completion of experiment for the inoculated: (f) and (g) straw column; (h) digestate column; and (i) and (j) manure compost column.



rate. Dissolution was controlled by both transport and interface reactions, the slowest process being rate-controlling⁶⁰. The initial rapid silicate dissolution of fine particles or high surface energy sites⁶⁰, was likely limited by the transport of column products away from the reaction sites. As the reactive sites were consumed or unreactive biproducts were produced, interface reactions likely became limiting.

The potential role of the microbes in maintaining greater dissolution in the inoculated columns was multi-fold. The production of siderophores and other chelators in the biotic columns, may have helped maintain a greater cation imbalance for example. While also acting to maintain the reactive surface through the inhibition of unreactive reaction products. The role of the microbes is discussed in more detail below.

Table 4 | Phospholipid fatty acid (PLFA) derived biomass (nmol g⁻¹ soil) and 2-Way ANOVA summary

	Bacteria	Fungi	Total	Fungi:Bacteria Ratio	Δ Total
Biotic Straw	0.54 ± 0.17	1.48 ± 0.60	2.02 ± 0.77	2.62 ± 0.48	1.17 ± 0.56
Abiotic Straw	0.44 ± 0.10	0.42 ± 0.14	0.85 ± 0.25		
Biotic Digestate	0.45 ± 0.06	0.53 ± 0.12	0.98 ± 0.15	1.19 ± 0.23	0.05 ± 0.01
Abiotic Digestate	0.49 ± 0.06	0.44 ± 0.10	0.93 ± 0.21		
Biotic Manure Compost	0.32 ± 0.07	0.10 ± 0.02	0.42 ± 0.09	0.33 ± 0.09	0.14 ± 0.09
Abiotic Manure Compost*	0.26	0.02	0.28		
Source of Variation	% of total	P value			
Interaction	15.9	0.0926			
Organic Carbon Source	41.2	0.0005			
Taxa	12.5	0.0455			

*no replicates to calculate standard deviation, due to sample contamination. Standard deviation of Δ Total was calculated as $a^2 + b^2 = c^2$, except biotic manure where it was carried through from Total.

The saturation of dissolution products in sediment and soil pores in marine olivine weathering studies have found pore saturation occurs within approximately 20 days, resulting in decreasing dissolution rates⁵³. Transport of the dissolution products away from the mineral surfaces, as in flow through column experiments like this, may help address the transportation issues which produces decreasing dissolution rates associated with saturation of olivine weathering reaction productions.

The increased weathering of the olivine in the biotic systems, in comparison to the abiotic controls, reflects similar results in flow-through experiments utilising albite and *Knufia petricola* fed with sterile nutrient solution⁶¹. *Knufia petricola* inoculation resulted in increased weathering, the growth of which and the formation of biofilms was enhanced in mixed cultures, further enhancing the dissolution of calcium⁶¹. The potential for symbiotic relationships to promote biofilm formation and microbially driven weathering, was the basis for using a mixed culture in this study. Single culture mineral dissolution experiments have already widely reported the ability of the fungi and bacteria utilised to weather silicate rocks^{25,31,33,38,39,42,45}. The potential and extent for symbiosis should be addressed in future work.

Flow through column experiments, utilising microbially inoculated minerals, have produced mixed results in terms of biotically enhanced weathering. The microbial effect on the weathering of diopside utilising heterotrophic bacterium *Pseudomonas Reactants* and the soil fungus *Chaetomium Brasiliense* was weak, with the acceleration in dissolution solely due to a decrease in pH in the porewaters⁴⁰. Further studies have found that the solubilisation and binding of significant amounts of Fe released during the dissolution of Fe-bearing olivine by wild-type *Knufia petricola* accelerated olivine dissolution in comparison to abiotic treatments³⁸. Due to the efficient prevention of Fe oxidation at the mineral surface, mediated by wild type-specific extracellular polymeric substances³⁸. In this study we also saw a weak effect of microbes on olivine dissolution in the columns containing digestate and manure compost as organic carbon sources, however a significant increase in dissolution was observed in the biotic columns utilising straw where PLFA microbial biomass was highest. This highlights the importance of selecting a combination of highly weathering microbes and an organic carbon source that can sustain extensive microbial growth and colonisation of mineral grains, to maximise the potential of microbially enhanced silicate weathering.

It was difficult to associate all inorganic carbon (TIC) in the columns and leachate to the sequestration of carbon from the atmosphere, and not driven by microbial respiration or the breakdown of the organic carbon source. It may be that the additional CO₂ released due to respiration was greater than the inorganic carbon sequestered. The released DOC that was not consumed by the microbes, furthermore, has the potential to be respired in the receiving environment.

The strong relationship between total alkalinity release rate and DIC in the leachate throughout the experiment (Fig. 3b), suggests there was a

relationship between the dissolution of the olivine and inorganic carbon captured in the leachate. This relationship strengthened when the day 4 abiotic straw columns were excluded, likely due to the contribution of DOC to total alkalinity. DOC can have a non-negligible influence on total alkalinity⁵⁶, due to the presence of carboxyl groups⁶². The average of the day 4 biotic straw samples fall along the linear regression (Fig. 3b), suggesting the DOC contribution in the straw columns proportionally influenced the total alkalinity and therefore weathering rate, similarly to the DOC produced by the digestate and manure compost columns.

Carbon isotope analyses and CO₂ flux measurements, in future experiments, could enable the differentiation of the inorganic carbon pools, based on microbial respiration of the organic carbon source, and atmospheric carbon⁶³. As evident in the increase in DIC and SIC in the biotic systems (Fig. 4b and Table 3), however, the inoculation of olivine with mixed fungi and bacterial cultures, resulted in an increase in inorganic carbon stored both in the column and the leachate. These results were statistically significant, as evidenced in the 2-Way ANOVA analyses of the column composition and time, and organic carbon source and inoculation status (Table 3). This provides encouragement for further investigation of silicate weathering bioreactors for inorganic carbon sequestration.

Many microbial weathering processes require direct contact, for example through the formation of biofilms, with the mineral surface^{18,22–25}. The extensive biofilm formation of both the organic carbon source and the mineral grains, and statistically significant larger PLFA biomass (Table 3), in the biotic straw columns was evidence to the increased production of total alkalinity being driven by microbial processes (i.e., oxidoreduction and complexolysis). The increased colonisation of the mineral grains in the straw columns may have been driven by the lower iron mass present in the straw, compared to the other organic carbon sources (Table 2), as the microbes were driven to break down the olivine to access iron. Oxidoreduction and complexolysis reactions, require direct contact to the mineral surface, for example through the formation of biofilms for electron transfer and nutrient extraction via excreted and/or membrane-associated molecules such as siderophores^{18,22–25,27}. While microbial respiration produces CO₂ leading to further mineral weathering through the formation of carbonic acid²⁸.

The increase in microbial growth did not appear to be dependent on the presence of major nutrients, such as nitrogen and phosphorus (Fig. 7), as the columns all became nutrient limited at about 25 days. Ammonium was indistinguishable between all the columns, while the digestate provided phosphate masses an order of magnitude greater than the manure and straw. The decrease in nitrate mass in the biotic columns for the first 2 weeks, in comparison to their abiotic controls, was likely due to the consumption of nitrate by the microbes. This does not explain the increased biofilm formation in the straw columns in comparison to the digestate and manure columns, however, as the straw did not release more nitrate than the other organic carbon sources.

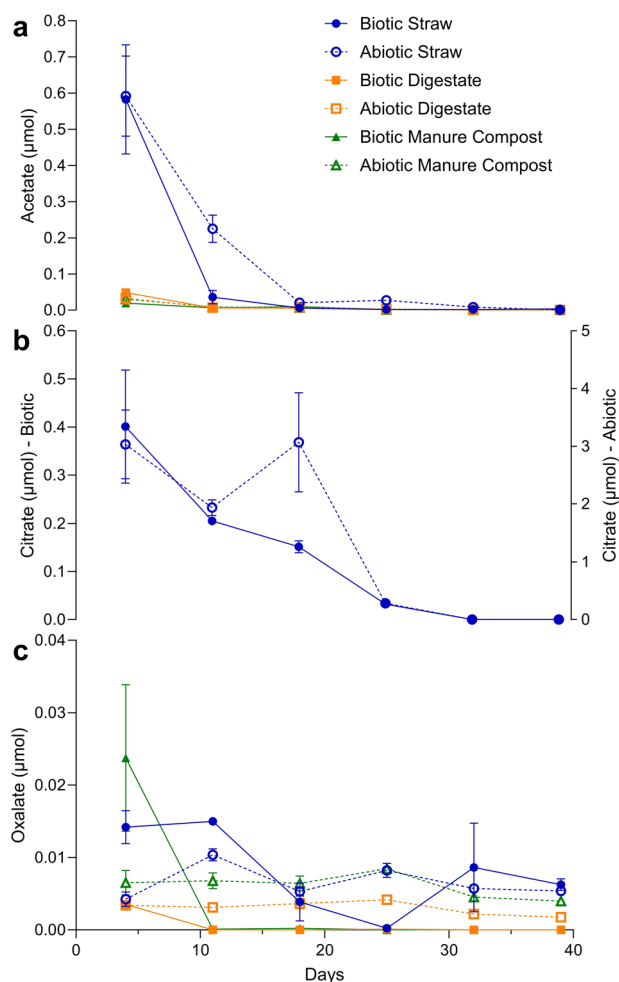


Fig. 6 | Low molecular weight organic acid moles through time. **a** Acetate, **(b)** citrate and **(c)** oxalate moles, and standard deviation, in the leachate each week. Citrate was not detected in the digestate or manure compost samples.

Labile organic carbon (DOC), or bioavailable carbon, appears to determine the extent of the biofilm formation. This was unsurprising given that the availability of simple labile carbon energy sources to microbes results in increased microbial respiration (i.e., microbial activity), which was further enhanced by a range of organic carbon sources of varying complexity⁶⁴. The controlled addition of simple bioavailable nitrogen and/or phosphorus could further increase microbial growth and mineral colonisation, and subsequent weathering. This requires further investigation, to ensure sequestered CO₂ was not offset by more potent greenhouse gases, such as N₂O.

The abiotic control and inoculated columns were stored and worked upon separately under sterile conditions, however, the frequency with which they were worked upon could have resulted in contamination. Any potential contamination did not, however, appear to affect the differences in weathering rates between the biotic and abiotic columns. Further, PLFA analyses did not show fungal or bacterial growth in the abiotic control columns. Fluorescence in situ hybridisation (FISH) staining could be used in future experiments to assess whether the biofilms were stable communities working synergistically to promote bio-weathering or a single species dominated and was primarily responsible for the bio-weathering. Similarly, sequencing could be used to provide more extensive analysis of the column microbiome and the relative abundances of the inoculated species and potential sources of contamination.

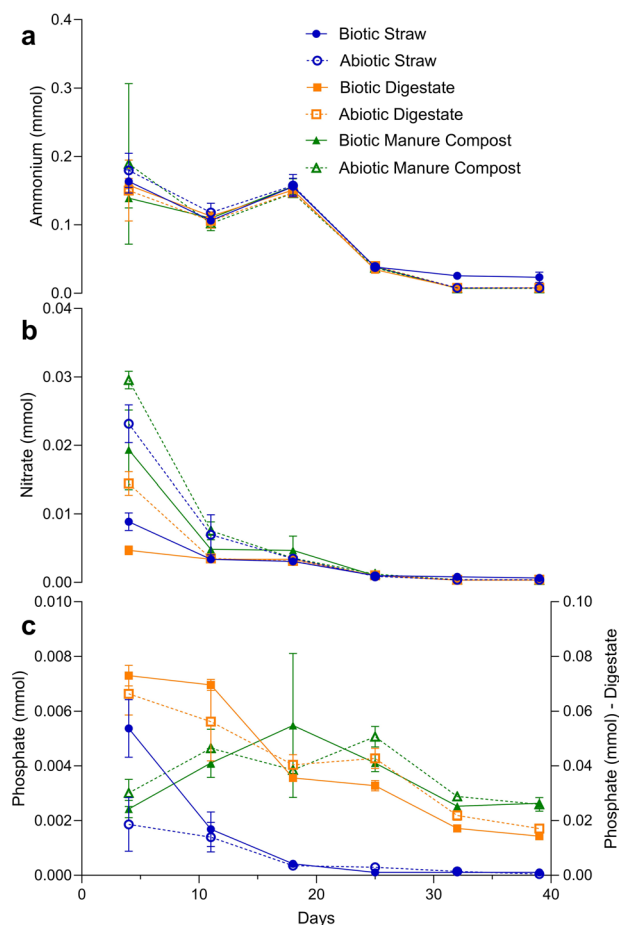


Fig. 7 | Nutrient moles through time. Moles of **(a)** ammonium, **(b)** nitrate, and **(c)** phosphate present in the leachate each week. Error bars represent standard deviation.

Low molecular weight organic acids (LMWOAs) are often purported as tools employed by microbes for the dissolution of silicate minerals^{19,26}. The presence of citrate, acetate and oxalate in the leachate of the columns in this experiment, was not enhanced by the presence of silicate weathering microbes which may utilise LMWOAs as a dissolution mechanism (Fig. 6). All biotic columns produced lower masses of the LMWOAs tested than the respective abiotic controls, suggesting the LMWOAs present in the leachate were released from the organic carbon sources themselves. The straw columns produced the largest citrate and acetate masses in the leachate. The decrease in the biotic straw columns, compared to the abiotic straw controls, of citrate and acetate may have been due to the consumption of the acids by the fungi and bacteria. Straw has been demonstrated as a source of LMWOAs when incorporated into soils⁶⁵, and acetate (conjugate base of acetic acid) was regularly used as a food source to support microbes in bioreactor technologies for nitrate removal and biogas generation^{66,67}.

Citrate also has a strong complexation tendency with tri- and divalent metal cations (e.g., Fe³⁺ and Mg²⁺)⁶⁸, forming metal colloids which would not be analysed via ion chromatography (measured dissolved species). The increase in magnesium, as a result of increased weathering, in the biotic straw columns, could result in greater complexation and less free citrate in the leachate. The complexation could also lower the saturation state of the dissolved magnesium, further promoting the dissolution of magnesium²⁰. Analysis via ICP-MS of acidified leachate samples for the total magnesium, could provide an estimate of the total complexed magnesium (i.e., the difference between the ICP-MS and IC magnesium masses).

The low LMWOA masses of the biotic columns, compared to the respective abiotic controls, does not mean that LMWOAs were not produced by the fungi and bacteria communities, to weather the olivine.

Localised decreases in pH in mineral pore spaces due to the formation of LMWOAs by microbes may not translate measurably to their overall mass in the leachate⁴⁰. The conditions, furthermore, were not optimised to encourage the microbes to produce LMWOAs. For example, the optimum pH for *Aspergillus niger* to produce citric acid was between 2.5–3.5⁶⁹. The pH of the leachate in this system was between 7 and 8 (Supplementary Fig. 1). Optimising the conditions of the columns (i.e., the addition of acid to decrease pH), to encourage LMWOA formation, is unlikely to be a viable solution to increasing microbially produced organic acids and acid induced weathering because of the increased energy (and therefore carbon emissions) associated with monitoring pH, producing and storing the acids, and addition of the acids to the weathering system.

Geophysical concerns of the application of olivine for *in natura* weathering in coastal and terrestrial ecosystems, such as increases in suspended particle matter, clogging of sediment pore spaces, smothering, and the release of toxic metals⁵³, are not largely relevant to *ex natura* silicate weathering bioreactors where aqueous column products and not solid reactants are dispersed/discharged into the environment.

The large-scale implementation of silicate weathering bioreactors, and the discharge of the biological and chemical column products could have significant effects on receiving ecosystems. Discharge of microbial species to waterways or soils could alter microbial community structure and function, and the wider ecosystem⁷⁰, thus paramount to column design and the successful implementation of a bioreactor is the careful selection of microbial species for column inoculation. Whereby considerations are made not only to the potential to enhance silicate weathering but the pathogenicity, presence, and abundance of the species in the receiving environments.

Discharge of highly alkaline waters to rivers and coastal ecosystems are desired for climate engineering⁵³, they could also play a role in offsetting ocean acidification⁷¹. The extent to which discharge from silicate weathering bioreactors could offset ocean acidification, however, requires further study and the development of large-scale columns. Primary production stimulation in receiving waters by the addition of silicon and iron olivine dissolution products could promote additional carbon sequestration^{53,72}. If the organic matter produced reaches the ocean, it can be stored for thousands to millions of years in ocean sediments if left undisturbed⁷³, however decomposition of the organic matter once it dies and falls through the water column, before it reaches the ocean floor, consumes oxygen, risking the development of eutrophic and hypoxic zones⁷⁴. The increased flux of toxic metals, such as nickel, from the dunite (olivine) mineral matrix could have considerable well established ecotoxicological consequences. Increased fluxes in organic carbon from the columns may also have positive ecological, and public health consequences. For example, the increased complexation of toxic metal species such as aluminium and subsequent decrease in bioavailability⁷⁵.

In this study we sought to establish the importance and efficacy of the organic carbons source to support microbial silicate weathering of dunite (forsterite olivine), and subsequent CO₂ sequestration, in small-scale flow through bioreactors. A mixture of dunite and three different widely available cheap organic carbon sources. The production of inorganic carbon was as follows: biotic straw > abiotic straw > biotic digestate > abiotic digestate > abiotic manure compost ≥ biotic manure. The enhanced weathering of the forsterite, and inorganic carbon production, in the microbially inoculated columns, compared to their abiotic controls, demonstrates it is worthwhile to continue investigating and developing microbial silicate weathering as carbon dioxide removal strategies. Further investigation of the optimal conditions (e.g., mineral size and type, biology, microbial synergies, watering frequency and volume, and nutrient supplementation) is required. In combination with considerations to the environmental consequences, positive and negative, of discharging column products into waterways or onto soils. This study focused on the short-term effects of microorganisms on the weathering of dunite and carbon sequestration in simple flow-through columns. Further studies are required to determine the extent to

which the dunite is altered long-term by the inoculation of bacteria and fungi in simple flow-through columns.

Reporting summary

Further information on research design is available in the Nature Research Reporting Summary linked to this article.

Data availability

All data analysed during this study are included in this published article [and its supplementary information files]. The datasets used and analysed during the current study available from the corresponding author on request.

Received: 1 December 2023; Accepted: 15 March 2024;

Published online: 02 April 2024

References

1. Rockström, J. et al. A roadmap for rapid decarbonization. *Science* **355**, 1269–1271 (2017).
2. UNFCCC. Paris Agreement (United Nations, 2015).
3. Gasser, T., Guivarch, C., Tachiiri, K., Jones, C. D. & Ciais, P. Negative emissions physically needed to keep global warming below 2 °C. *Nat. Commun.* **6**, 7958 (2015).
4. Fuss, S. et al. Negative emissions—Part 2: costs, potentials and side effects. *Environ. Res. Lett.* **13** <https://doi.org/10.1088/1748-9326/aabf9f> (2018).
5. Vicca, S. et al. Is the climate change mitigation effect of enhanced silicate weathering governed by biological processes? *Glob. Change Biol.* 711–726 <https://doi.org/10.1111/gcb.15993> (2021).
6. IPCC. *Climate Change 2022: Mitigation of Climate Change. Contribution of Working Group III to the Sixth Assessment Report of the Intergovernmental Panel on Climate Change* (Cambridge University Press, 2022).
7. Smith, S. M. et al. *The State of Carbon Dioxide Removal 1st Edition* (The State of Carbon Dioxide Removal, 2023).
8. Walker, J. C. G., Hays, P. B. & Kasting, J. F. A negative feedback mechanism for the long-term stabilization of Earth's surface temperature. *J. Geophys. Res. Oceans* **86**, 9776–9782 (1981).
9. Berner, R. A., Lasaga, A. C. & Garrels, R. M. The carbonate-silicate geochemical cycle and its effect on atmospheric carbon dioxide over the past 100 million years. *Am. J. Sci.* **283**, 641–683 (1983).
10. Beerling, D. J. et al. Potential for large-scale CO₂ removal via enhanced rock weathering with croplands. *Nature* **583**, 242–248 (2020).
11. Hartmann, J. et al. Enhanced chemical weathering as a geoengineering strategy to reduce atmospheric carbon dioxide, supply nutrients, and mitigate ocean acidification. *Rev. Geophys.* **51**, 113–149 (2013).
12. Finlay, R. D. et al. Reviews and syntheses: biological weathering and its consequences at different spatial levels – from nanoscale to global scale. *Biogeosciences* **17**, 1507–1533 (2020).
13. Brundrett, M. C. & Tedersoo, L. Evolutionary history of mycorrhizal symbioses and global host plant diversity. *N. Phytol.* **220**, 1108–1115 (2018).
14. Rosling, A. Trees, mycorrhiza and minerals –field relevance of in vitro experiments. *Geomicrobiol. J.* **26**, 389–401 (2009).
15. Tunlid, A., Floudas, D., Op De Beeck, M., Wang, T. & Persson, P. Decomposition of soil organic matter by ectomycorrhizal fungi: mechanisms and consequences for organic nitrogen uptake and soil carbon stabilization. *Front. For. Glob. Change* **5** <https://doi.org/10.3389/ffgc.2022.934409> (2022).
16. Angers, D. A. & Caron, J. Plant-induced changes in soil structure: processes and feedbacks. *Biogeochemistry* **42**, 55–72 (1998).
17. Van Groenigen, J. W. et al. How fertile are earthworm casts? A meta-analysis. *Geoderma* **338**, 525–535 (2019).

18. Uroz, S., Calvaruso, C., Turpault, M.-P. & Frey-Klett, P. Mineral weathering by bacteria: ecology, actors and mechanisms. *Trends Microbiol.* **17**, 378–387 (2009).
19. Kirtzel, J. et al. Organic acids, siderophores, enzymes and mechanical pressure for black slate bioweathering with the basidiomycete *Schizophyllum commune*. *Environ. Microbiol.* **22**, 1535–1546 (2020).
20. Hoffland, E. et al. The role of fungi in weathering. *Front. Ecol. Environ.* **2**, 258–264 (2004).
21. Adebayo, A. A., Harris, R. F. & Gardner, W. R. Turgor pressure of fungal mycelia. *Trans. Br. Mycol. Soc.* **57**, 145–151 (1971).
22. Leyval, C. & Berthelin, J. Interactions between *Laccaria laccata*, *Agrobacterium radiobacter* and beech roots: Influence on P, K, Mg, and Fe mobilization from minerals and plant growth. *Plant Soil* **117**, 103–110 (1989).
23. Hernandez, M. E., Kappler, A. & Newman, D. K. Phenazines and other redox-active antibiotics promote microbial mineral reduction. *Appl. Environ. Microbiol.* **70**, 921–928 (2004).
24. Newman, D. K. How bacteria respire minerals. *Science* **292**, 1312–1313 (2001).
25. Olsson-Francis, K., VAN Houdt, R., Mergeay, M., Leys, N. & Cockell, C. S. Microarray analysis of a microbe-mineral interaction. *Geobiology* **8**, 446–456 (2010).
26. Welch, S. A. & Ullman, W. J. The effect of organic acids on plagioclase dissolution rates and stoichiometry. *Geochim. Cosmochim. Acta* **12**, 2725–2736, (1993).
27. Welch, S. A., Taunton, A. E. & Banfield, J. F. Effect of microorganisms and microbial metabolites on apatite dissolution. *Geomicrobiol. J.* **19**, 343–367 (2002).
28. Lian, B., Chen, Y., Zhu, L. & Yang, R. Effect of microbial weathering on carbonate rocks. *Earth Sci. Front.* **15**, 90–99 (2008).
29. Johnson, D. B. Biomining—biotechnologies for extracting and recovering metals from ores and waste materials. *Curr. Opin. Biotech.* **30**, 24–31 (2014).
30. Rawlings, D. E. & Silver, S. Mining with microbes. *Nat. Biotechnol.* **13**, 773–778 (1995).
31. Song, W., Ogawa, N., Oguchi, C. T., Hatta, T. & Matsukura, Y. Effect of *Bacillus subtilis* on granite weathering: a laboratory experiment. *CATENA* **70**, 275–281 (2007).
32. Wallander, H. & Wickman, T. Biotite and microcline as potassium sources in ectomycorrhizal and non-mycorrhizal *Pinus sylvestris* seedlings. *Mycorrhiza* **9**, 25–32 (1999).
33. Gerrits, R. et al. High-resolution imaging of fungal biofilm-induced olivine weathering. *Chem. Geol.* **559**, 119902 (2021).
34. Li, Z., Liu, L., Chen, J. & Teng, H. H. Cellular dissolution at hypha- and spore-mineral interfaces revealing unrecognized mechanisms and scales of fungal weathering. *Geology* **44**, 319–322 (2016).
35. Wild, B., Gerrits, R. & Bonneville, S. The contribution of living organisms to rock weathering in the critical zone. *npj Mat. Degrad.* **6**, 98 (2022).
36. Zhou, X., Shen, Y., Fu, X. & Wu, F. Application of sodium silicate enhances cucumber resistance to fusarium wilt and alters soil microbial communities. *Front. Plant. Sci.* **9**, 624–624 (2018).
37. ten Berge, H. F. M. et al. Olivine weathering in soil, and its effects on growth and nutrient uptake in ryegrass (*Lolium perenne* L.): a pot experiment. *PLoS One* **7**, e42098 (2012).
38. Gerrits, R. et al. How the rock-inhabiting fungus *K. petricola* A95 enhances olivine dissolution through attachment. *Geochim. Cosmochim. Acta* **282**, 76–97 (2020).
39. Wang, W., Sun, J., Dong, C. & Lian, B. Biotite weathering by *Aspergillus niger* and its potential utilisation. *J. Soils Sediment.* **16**, 1901–1910 (2016).
40. Pokrovsky, O. S., Shirokova, L. S., Zabelina, S. A., Jordan, G. & Bénéžeth, P. Weak impact of microorganisms on Ca, Mg-bearing silicate weathering. *npj Mat. Degrad.* **5**, 51 (2021).
41. Van Noort, R., Mørkved, P. T. & Dundas, S. H. Acid neutralization by mining waste dissolution under conditions relevant for agricultural applications. *Geosci* **8**, 380 (2018).
42. Cockell, C. S. et al. Space station biomining experiment demonstrates rare earth element extraction in microgravity and Mars gravity. *Nat. Commun.* **11**, 5523 (2020).
43. Tessei, D. et al. Draft genome sequences of the black rock fungus *knufia petricola* and its spontaneous nonmelanized mutant. *Genome Announc* **5**, e01242–01217 (2017).
44. Cairns, T. C., Nai, C. & Meyer, V. How a fungus shapes biotechnology: 100 years of *Aspergillus niger* research. *Fungal Biol. Biotech.* **5**, 13 (2018).
45. Byloos, B. et al. The impact of space flight on survival and interaction of *cupriavidus metallidurans* CH34 with Basalt, a volcanic moon analog rock. *Front. Microbiol.* **8**, 671 (2017).
46. ABAS. Committee for Biological Agents, Technical Rules for Biological Agents - Classification of Prokaryotes (Bacteria and Archaea) into Risk Groups. 5–252 (Federal Institute for Occupational Safety and Health 2010).
47. Noack-Schönmann, S. et al. Genetic transformation of *Knufia petricola* A95—a model organism for biofilm-material interactions. *AMB Express* **4**, 80 (2014).
48. Nai, C. et al. Nutritional physiology of a rock-inhabiting, model microcolonial fungus from an ancestral lineage of the Chaetothiales (Ascomycetes). *Fungal Genet. Biol.* **56**, 54–66 (2013).
49. Novozamsky, I., van Eck, R., Houba, V. J. G. & van der Lee, J. J. Solubilization of plant tissue with nitric acid-hydrofluoric acid-hydrogen peroxide in a closed-system microwave digester. *Commun. Soil Sci. Plant Anal.* **27**, 867–875 (1996).
50. Joergensen, R. G. Phospholipid fatty acids in soil—drawbacks and future prospects. *Biol. Fertil. Soils* **58**, 1–6 (2022).
51. Joergensen, R. G. & Wichern, F. Quantitative assessment of the fungal contribution to microbial tissue in soil. *Soil Biol. Biochem.* **40**, 2977–2991 (2008).
52. Amann, T., Hartmann, J., Hellmann, R., Pedrosa, E. T. & Malik, A. Enhanced weathering potentials—the role of in situ CO₂ and grain size distribution. *Front. Clim.* **4**, <https://doi.org/10.3389/fclim.2022.929268> (2022).
53. Montserrat, F. et al. Olivine dissolution in seawater: implications for CO₂ sequestration through enhanced weathering in coastal environments. *Environ. Sci. Technol.* **51**, 3960–3972 (2017).
54. Wolf-Gladrow, D. A., Zeebe, R. E., Klaas, C., Körtzinger, A. & Dickson, A. G. Total alkalinity: the explicit conservative expression and its application to biogeochemical processes. *Mar. Chem.* **106**, 287–300 (2007).
55. Vienne, A. et al. Soil carbon sequestration and the role of earthworms in an enhanced weathering mesocosm experiment. *Available at SSRN 4449286*
56. Kerr, D. E., Brown, P. J., Grey, A. & Kelleher, B. P. The influence of organic alkalinity on the carbonate system in coastal waters. *Mar. Chem.* **237**, 104050 (2021).
57. Song, S., Bellerby, R. G. J., Wang, Z. A., Wurgaft, E. & Li, D. Organic Alkalinity as an important constituent of total alkalinity and the buffering system in river-to-coast transition zones. *J. Geophys. Res. Oceans* **128**, e2022JC019270 (2023).
58. Dickson, A. G., Sabine, C. L. & Christian, J. R. *Guide to best practices for ocean CO₂ measurements* PICES Special Publication 3. (2007).
59. Wild, B., Imfeld, G., Guyot, F. & Daval, D. Early stages of bacterial community adaptation to silicate aging. *Geology* **46**, 555–558 (2018).
60. Brantley, S. L. Kinetics of mineral dissolution. In *Kinetics of Water-Rock Interaction* (ed James D. Kubicki Susan L. Brantley, Art F. White) Ch. 5, 151–210 (Springer, 2007).
61. Seiffert, F., Bandow, N., Bouchez, J., von Blanckenburg, F. & Gorbushina, A. A. Microbial colonization of bare rocks: laboratory

- biofilm enhances mineral weathering. *Proc. Earth Planet. Sci.* **10**, 123–129 (2014).
62. Hertkorn, N. et al. Characterization of a major refractory component of marine dissolved organic matter. *Geochim. Cosmochim. Acta* **70**, 2990–3010 (2006).
63. Min, K., Lehmeier, C. A., Iv, F. B. & Billings, S. A. Carbon availability modifies temperature responses of heterotrophic microbial respiration, carbon uptake affinity, and stable carbon isotope discrimination. *Front. Microbiol.* **7**, <https://doi.org/10.3389/fmicb.2016.02083> (2016).
64. Numa, K. B., Robinson, J. M., Arcus, V. L. & Schipper, L. A. Separating the temperature response of soil respiration derived from soil organic matter and added labile carbon compounds. *Geoderma* **400**, 115128 (2021).
65. Shan, Y., Cai, Z., Han, Y., Johnson, S. E. & Buresh, R. J. Organic acid accumulation under flooded soil conditions in relation to the incorporation of wheat and rice straws with different C:N ratios. *Soil Sci. Plant Nutr.* **54**, 46–56 (2008).
66. Roser, M. B. et al. Carbon dosing increases nitrate removal rates in denitrifying bioreactors at low-temperature high-flow conditions. *J. Environ. Qual.* **47**, 856–864 (2018).
67. Westerholm, M., Moestedt, J. & Schnürer, A. Biogas production through syntrophic acetate oxidation and deliberate operating strategies for improved digester performance. *Appl. Energy* **179**, 124–135 (2016).
68. Glusker, J. P. Citrate conformation and chelation: enzymic implications. *Acc. Chem. Res.* **13**, 345–352 (1980).
69. Show, P. L. et al. Overview of citric acid production from *Aspergillus niger*. *Front. Life Sci.* **8**, 271–283 (2015).
70. Trabelsi, D. & Mhamdi, R. Microbial inoculants and their impact on soil microbial communities: a review. *Biomed. Res. Int.* **2013**, 863240 (2013).
71. Middelburg, J. J., Soetaert, K. & Hagens, M. Ocean Alkalinity, buffering and biogeochemical processes. *Rev. Geophys.* **58**, e2019RG000681 (2020).
72. Hauck, J., Köhler, P., Wolf-Gladrow, D. & Völker, C. Iron fertilisation and century-scale effects of open ocean dissolution of olivine in a simulated CO₂ removal experiment. *Environ. Res. Lett.* **11**, 024007 (2016).
73. Estes, E. R. et al. Persistent organic matter in oxic seafloor sediment. *Nat. Geosci.* **12**, 126–131 (2019).
74. Allaby, M. Eutrophication. in *A Dictionary of Ecology* (Oxford University Press, 2010).
75. McCartney, A. G. et al. Long-term trends in pH, aluminium and dissolved organic carbon in Scottish fresh waters; implications for brown trout (*Salmo trutta*) survival. *Sci. Total Environ.* **310**, 133–141 (2003).

Acknowledgements

We would like to thank Christoffer Bergval for his assistance with analytical instrumentation and Veera Nogerius for her support setting up the experiments and culturing. We would also like to thank Yanzhang Luo from MAGNETic resonance research facility (MAGNEFY, Wageningen University) for running the NMR samples. This research was supported by the European

Commission: H2020 FET-open project Super Bio-Accelerated Mineral weathering: a new climate risk hedging column technology' — 'BAM' (grant agreement number 964545).

Author contributions

T.D.W.C.: paper writing; statistical analyses; experimental design; experiment operation; experimental analyses. M.W.: experimental design; experiment operation; ph, conductivity, ion chromatography, scanning electron microscopy analyses. A.R.: experimental design; editing. T.C.: Carbon source composition analyses; editing. R.P.: mineral surface area and composition analyses; editing. H.N.: experimental design; editing. M.H.: experimental design; editing; funding. A.V.: experimental design; editing; funding. J.W.V.G.: experimental design; editing; funding. J.H.: experimental design; editing; funding. I.A.J.: experimental design; funding. L.R.: editing. E.S.: experimental design; funding. M.V.T.: experimental design; editing. S.E.V.: experimental design; editing; funding. S.V.: experimental design; statistical analyses; editing; funding. A.N.: experimental design; editing; funding; scanning electron microscopy analysis; paper writing.

Funding

Open access funding provided by Uppsala University.

Competing interests

The authors declare no competing interests.

Additional information

Supplementary information The online version contains supplementary material available at <https://doi.org/10.1038/s41529-024-00454-w>.

Correspondence and requests for materials should be addressed to Thomas D. W. Corbett.

Reprints and permissions information is available at <http://www.nature.com/reprints>

Publisher's note Springer Nature remains neutral with regard to jurisdictional claims in published maps and institutional affiliations.

Open Access This article is licensed under a Creative Commons Attribution 4.0 International License, which permits use, sharing, adaptation, distribution and reproduction in any medium or format, as long as you give appropriate credit to the original author(s) and the source, provide a link to the Creative Commons licence, and indicate if changes were made. The images or other third party material in this article are included in the article's Creative Commons licence, unless indicated otherwise in a credit line to the material. If material is not included in the article's Creative Commons licence and your intended use is not permitted by statutory regulation or exceeds the permitted use, you will need to obtain permission directly from the copyright holder. To view a copy of this licence, visit <http://creativecommons.org/licenses/by/4.0/>.

© The Author(s) 2024